# Finite Element Analysis of Ceramic Abutment–Restoration Combinations for Osseointegrated Implants

*George Papavasiliou, DDS, MS**
*Aris Petros D. Tripodakis, DDS, MS, Dr Odont***
*Phophi Kamposiora, DDS, MS****
*Jorg Rudolf Strub, DMD, PhD*****
*Stephen C. Bayne, MS, PhD, FADM******

All-ceramic restorations can solve many esthetic problems associated with implant-supported prostheses. This study evaluated stress concentration and distribution in implant abutments under normal masticatory forces using computer simulations. Two-dimensional finite element analysis was used to study four different abutment–restoration combinations using Brånemark implants. The models considered two positions of the fastening screw, two positions of the crown margins, cemented versus screw-retained prostheses, and clinical loads of 200 N. Models having screws on top of abutments had the lowest stresses (3.1 to 4.8 MPa) and best stress distribution. Screw-retained prostheses and short crown margins increased overall stresses (9.9 to 11.4 MPa). *Int J Prosthodont 1996;9:254–260.*

Appearance plays an important role in the lives of most people, especially professionals, and any restoration with less than optimal esthetics will probably not be acceptable. Osseointegrated dental implants have earned an excellent reputation for biocompatibility, predictability, and function throughout the past decade.[1–3] However, there is potential for esthetic improvement. Implant-supported prostheses rely heavily on metallic components (abutments, screws, overstructures) for strength in large, complete arch restorations such as those that are fixed-detachable.[4] For smaller restorations, especially single-tooth replacements, these may not be necessary. Single-tooth replacements involve smaller functional loads in the absence of cantilevers[5] and normal occlusal loads are shared with the adjacent natural teeth.

Ceramic materials are acceptable for veneering implant-supported prostheses,[4] and their use greatly improves the esthetics of implant restorations. Nevertheless the prostheses still have a metal framework that may cause esthetic problems at the cervical third of the prosthesis where the metal ceramic overstructure joins the implant.[6] The optical problem of metal ceramic implant restorations is the same as that of the conventional prosthesis.[7] All-ceramic restorations could solve these esthetic problems, but until recently dental ceramics lacked adequate strength. The introduction of sintered systems such as In-Ceram (Vita Zahnfabrik, Bad-Säckingen, Germany) provided dentistry with a stronger all-ceramic material[8] that could withstand the functional requirements of most small conventional or implant-supported prostheses.

The remaining problem for implant restorations is to minimize inaccuracies in prosthesis fit.[9] The fit of prefabricated (machined) implant components is

*Assistant Professor, Department of Prosthodontics, School of Dentistry, University of North Carolina at Chapel Hill, Chapel Hill, North Carolina.
**Assistant Professor, Department of Prosthodontics, School of Dentistry, University of Athens, Athens, Greece; Visiting Assistant Professor, Department of Prosthodontics, School of Dentistry, Albert Ludwigs University, Freiburg, Germany.
***Clinical instructor, Department of Prosthodontics, School of Dentistry, University of North Carolina at Chapel Hill, Chapel Hill, North Carolina.
****Professor and Chairman, Department of Prosthodontics, School of Dentistry, Albert Ludwigs University, Freiburg, Germany.
*****Professor, Section Head of Biomaterials, Department of Operative Dentistry, School of Dentistry, University of North Carolina at Chapel Hill, Chapel Hill, North Carolina.

**Reprint requests**: Dr George Papavasiliou, 25 Bouziani Str, 17234 Athens, Greece.

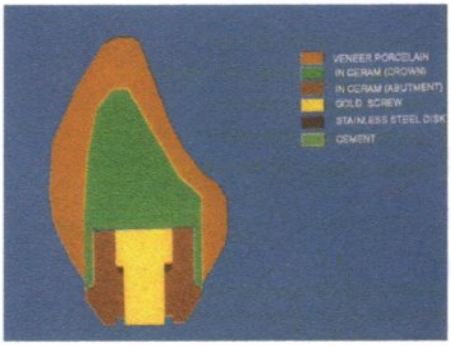


**Fig 1a** Two-dimensional schematic of model design for FEA model I.

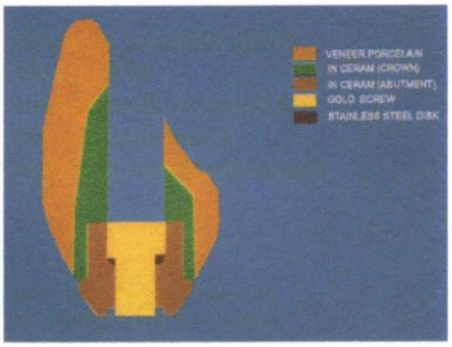


**Fig 1b** Two-dimensional schematic of model design for FEA model II.

usually excellent.[10] However, this has been less frequently found with cast overstructures. Inherent problems with casting techniques and castable materials[11] often necessitates sectioning and soldering of frameworks for implant-supported restorations to minimize misfit.

A copy-milling technique (Celay, Mikrona, Schreitenbach, Switzerland) has been proposed[6,12] to solve the problem of fit for ceramic abutment implant restorations. In this approach In-Ceram blocks are used to machine the framework of the restoration and provide an esthetic prosthesis, minimizing exposed metal components. The strength of these restorations is promising.[6]

The purpose of this study was to evaluate the mechanical behavior of four previously described[6] designs of copy-milled implant overstructures under normal masticatory forces using two-dimensional finite element analysis (FEA).

## Methods

Finite element analysis has found many applications in dental research during the last decade.[13,14] The method gives the operator the ability to simulate many situations with minor modifications of an initial computer model and without the time and expense required for the construction and testing of real life models. An overview of the method has been previously published.[15] This investigation used COSMOS/M FEA computer software (Version 1.65A, Structural Research and Analysis, Santa Monica, CA) to examine stress levels and distribution for two-dimensional (2D) computer models of osseointegrated implants restored with different abutment and restoration designs. Two-dimensional FEA offers good simulation for structures that are axisymmetric, as were most models in this study. Limitations of the method compared to three-dimensional (3D) FEA arise when nonaxisymmetric models are evaluated, and from the fact that only one plane of stress distribution is examined. Finite element analysis models can be loaded at any point and in any direction. A 200-N load was applied to all models in an oblique (45-degree) direction at the boundary between the occlusal and the middle thirds of the lingual surface. The loading angle and position were chosen to comply with those in the paper by Tripodakis et al,[6] where bench-top models with the same designs were tested. This was done to allow comparison of the results of the two studies.

A Brånemark implant (Nobelpharma USA, Westmont, IL) 11 mm long and 4 mm in diameter was modeled as being osseointegrated to normal cortical and cancellous bone. Four different abutment–restoration combinations were simulated as overstructures to the implant. The abutment designs varied, but the restoration geometries were as similar as possible so that resulting stress and stress distributions could be assigned to the abutment differences.

Two models (I, II) (Figs 1a and 1b) used a design[6] with a screw channel wide enough to contain the screw head within the abutment. A stainless steel disk was seated on an internal rounded shoulder by the screw head to help stabilize the abutment. An external rounded shoulder was placed at a level lower than the internal one to complete the design. For model I (Fig 1a), the shoulder was used as the margin for an all-ceramic crown cemented on the abutment. For model II (Fig 1b), ceramic veneering material was

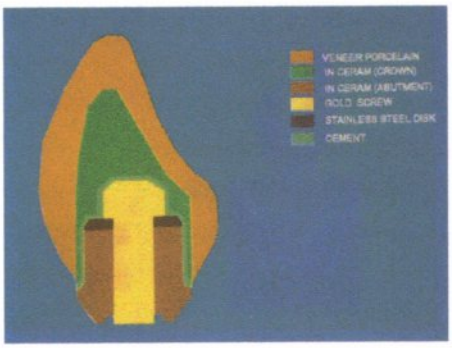


**Fig 1c** Two-dimensional schematic of model design for FEA model III.

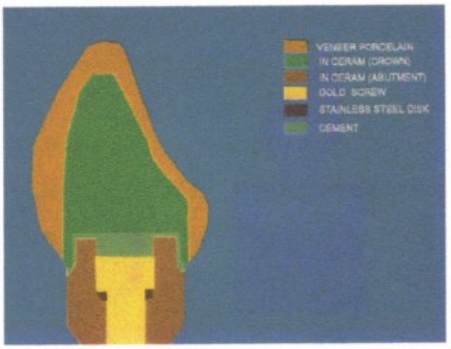


**Fig 1d** Two-dimensional schematic of model design for FEA model IV.

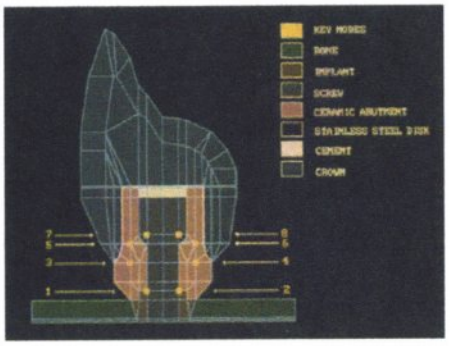


**Fig 2** Key nodes of interest for stress analysis: at the interface among the implant, the screw, and the ceramic abutment (1 and 2), at four points in the mass of the ceramic abutment (3, 4, 5, and 6), and at the internal corners of the screw head (7 and 8).

**Table 1** Mechanical Properties (Modulus, Poisson's Ratio) for Oral Tissues and Prosthetic Materials in FEA Evaluations

| Material | Modulus (E)(MPa) | Poisson's ratio ($\nu$) | Literature reference |
|---|---|---|---|
| Cortical bone | 13,700 | 0.30 | 18 |
| Cancellous bone | 7,930 | 0.30 | 19 |
| Titanium | 102,195 | 0.35 | 20 |
| Type III gold alloy | 91,000 | 0.35 | 21 |
| Feldspathic porcelain | 82,800 | 0.35 | 22 |
| Composite cement | 12,500 | 0.35 | 23 |
| In-Ceram | 364,000 | 0.33 | 24 |
| Stainless steel | 200,000 | 0.30 | 25 |

simulated as being fired directly onto the abutment. The screw access hole was left empty. In clinical situations the hole is filled with a thermoplastic material and sealed with resin composite, but this procedure does not contribute strength to the design.

In another abutment design (Fig 1c) the screw head was placed above the abutment so that an internal shoulder was not necessary. The screw head was used to fasten a stainless steel disk covering the occlusal end of the abutment. An all-ceramic crown was simulated as being cemented onto the abutment. The last model (Fig 1d) used an abutment design similar to models I and II, except for the use of an external rounded shoulder placed at a higher level than the internal design, which precluded the simulated cemented crown from embracing the area of the screw head.

The four models included from 313 to 376 elements. In this study, quadrilateral plane stress elements were used. The interfaces between materials were continuous. For each model, fixation of the bottom of the bone section was applied. The fixation was chosen away from the area of interest to avoid interferences with the results of the study. A convergence test was performed where the number of the elements was doubled and then tripled to assure the proper mesh density. For all three mesh densities stress distributions were practically identical, and stress values differed at the third or fourth decimal point. For ease of model construction the simplest mesh was used in the study. In each design the simulated crown was a maxillary central incisor luted using resin composite cement. All models were loaded at the boundary between the occlusal and the middle thirds of the palatal surface (see Fig 3). Young's modulus and Poisson's

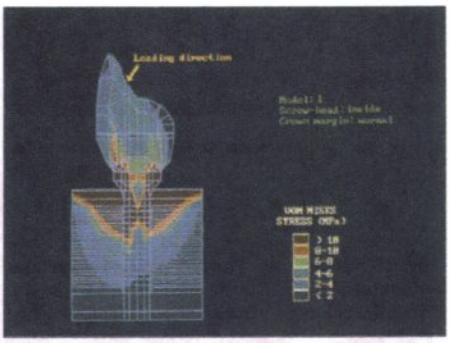


**Fig 3a** Stress contour plots for FEA model I.

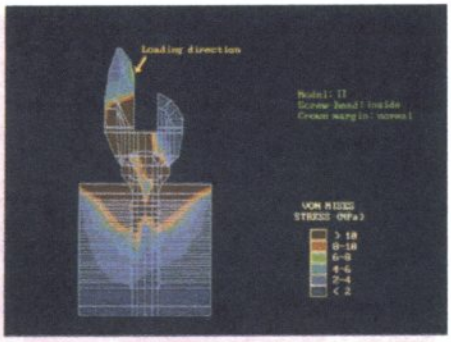


**Fig 3b** Stress contour plots for FEA model II.

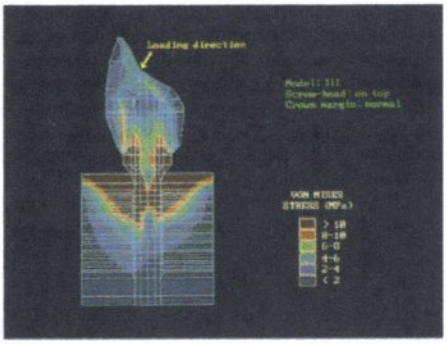


**Fig 3c** Stress contour plots for FEA model III.

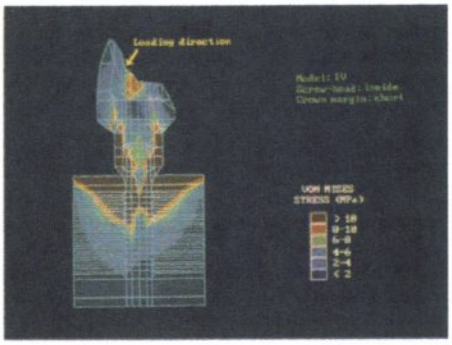


**Fig 3d** Stress contour plots for FEA model IV.

ratios were used to define the mechanical properties for each element in the simulated structures (Table 1).

Stresses and deformations were calculated for every node of each model with FEA. Reporting all this information would be beyond the purpose of this investigation. Stress plots typically are used[15] to provide an overview of the stress distribution and resolved stress levels involved. In addition to stress plots, stress values for specific nodes in regions of special interest were reported. These nodes (Fig 2) were located: at the interface along the implant, the screw, and the ceramic abutment (1 and 2) , at four points in the mass of the ceramic abutment, (3, 4, 5, and 6), and at the internal corners of the screw head (7 and 8) (Fig 2).

Stress levels were reported for each of the eight nodes according to the Von Mises criteria[16] (equivalent stress). This type of analysis is very helpful for FEA studies because it determines the total state of stress for the specific node.[15] The stresses reported in the results tables indicate the local sensitivity of each model to the applied loads.[17] The use of statistical analyses is very limited for FEA studies[4] because the results of the models' calculations are invariant.

## Results

Figures 3a to 3d represent the stress distributions for the four models. The stress plots are color coded. Corresponding resultant stress levels are given at the right of each plot.

**Table 2** Stress Values (MPa) for Specific Nodes for Models I to IV

| Key nodes | Location of key nodes | Model I | Model II | Model III | Model IV |
|---|---|---|---|---|---|
| 1 | Facial interface along fixture/screw/abutment | 8.0 | 7.5 | 6.6 | 8.1 |
| 2 | Lingual interface along fixture/screw/abutment | 7.1 | 9.0 | 7.2 | 7.1 |
| 3 | Facial internal corner of screw head | 6.2 | 11.4 | 3.1 | 5.7 |
| 4 | Lingual internal corner of screw head | 6.5 | 9.9 | 4.8 | 6.0 |
| 5 | Inside copy-milled ceramic abutment | 14.0 | 15.1 | 15.4 | 16.4 |
| 6 | Inside copy-milled ceramic abutment | 13.0 | 12.2 | 14.3 | 14.4 |
| 7 | Inside copy-milled ceramic abutment | 8.7 | 7.9 | 10.0 | 9.4 |
| 8 | Inside copy-milled ceramic abutment | 8.1 | 8.9 | 9.5 | 8.1 |

In model I (Fig 3a), stresses were concentrated in the cervical area of the restoration, just below the screw head and within the ceramic abutment. There was little stress in the crown except in the facial region of the cemented crown-abutment interface. There were high stresses concentrated in the gingival end of the implant and in the cortical bone surrounding that area.

In model II (Fig 3b), stresses were greater than for model I. High stresses occurred in the screw head, the restoration, and the abutment. The middle third of the facial region of the restoration in front of the screw access hole encountered the most stress and produced a diagonal stress distribution pattern toward the cervical of the palatal side. The stress patterns in the implant and the surrounding bone were similar to model I.

For model III (Fig 3c), stress patterns differed from those for model I in two areas. Stresses in the cervical area of the screw (where the screw head was located in model I) were lower by approximately 2 MPa. The same was true for the area around the screw head.

For model IV (Fig 3d), high stresses were concentrated along the area of the restoration not covered by the crown. That area included the cervical area of the abutment, the screw, and screw head. There was also more stress concentration in the crown at the point of load application and the facial surface.

The stresses at the nodes of interest are presented in Table 2. For nodes 1 and 2 (junction of implant/abutment/screw), stresses were similar for all models (6.6 MPa to 9.0 MPa), with the highest stresses reported for model II. For nodes 3 and 4 (inner corner of screw head) stress values varied among models. The lowest values (3.1 MPa to 4.8 MPa) were for model III, where the screw was placed on top of the abutment. The highest values (9.9 MPa to 11.4 MPa) were reported for model II and were 2 to 3 times higher than the ones for model III, and almost double the values for models I and IV. For nodes 5 to 8 (inside the ceramic abutment) stress values were similar for all models (7.9 MPa to 10.0 MPa).

## Discussion

The stress levels and distributions were grossly similar in spite of some notable differences among the four models. High stresses were always distributed to the superior portion of the implant and the surrounding cortical bone. High stresses always occurred in the prosthesis perimeter at the junction with the implant. Moderate stresses were associated with occlusal regions of the prosthesis where the loading originated. Low stresses were associated with the facial and palatal regions of the prosthesis that were formed using veneering porcelain. The major differences between models were associated with the region of prosthesis attachment to the implant.

All abutments were simulated as being made from the same material, so that the ones revealing the highest stresses would indicate sites more prone to fracture. The probability toward fracture was primarily governed by amount and location of stress. The most critical area was at the screw/implant/abutment junction (keynodes 1 through 4) where most failures occurred. Based on the stresses revealed by the prosthesis attachment to the implant and the interfacial values reported in Table 2, the order of susceptibility to fracture for the models was II > IV > I > III.

Models III and I had very similar and favorable stress distributions. High stress concentrations (8.1 MPa to 10.0 MPa) were still observed at the cervical part of the ceramic abutment. Model III showed less stress concentration around the screw and the screw head (3.1 to 4.8 MPa and 6.2 to 6.5 MPa, respectively) than model I. Placement of the screw head on top of the ceramic abutment had previously been suggested as resulting in more favorable stress distribution,[6] inasmuch as preloading would produce compression and thus negate any tensile stresses created during intraoral function. The predominantly ceramic abutment seemed to distribute stresses well. Although the screw was placed in a less favorable situation in model III than in model I (as a result of its increased length), this did not adversely affect the stress distribution.

In model IV the margin of the crown was located coronal to the level of the screw head. This resulted in greater stress concentration in the cervical area of the ceramic abutment versus models I and III. By not embracing the abutment, the crown exposed this area to potential tensile stresses that could be detrimental to the ceramic material. The stress levels were only slightly greater than for the other models, but the difference between model IV and models I or III was that greater stresses were concentrated more along the thinnest area of the abutment around the housing of the screw head.

Model II had the least favorable stress distribution. Greater stress occurred in the screw head (2 to 3 times higher than for the other models) and on the facial region of the restoration. This tended to produce a diagonal stress distribution pattern. This has been shown to be detrimental by Tripodakis et al,[6] who used fracture tests with similar abutments. In actual clinical situations there would not be a gap between the facial and lingual surfaces because the access hole for the screw has sidewalls. For that reason, evaluation of this model with 3D FEA could offer further understanding of the stress distribution.

The filling material that is usually a resin composite did not add to the integrity of the restoration.

## Conclusions

Within the parameters of the project design and within the limitations of two-dimensional finite element analysis the following conclusions can be made:

1. All designs produced maximum stresses in the coronal end of the implant, in cortical bone, and in the region of the abutment–restoration attachment.
2. Cemented restorations distributed less stress to weak areas of the abutments than those restorations that were screw retained.
3. Placement of the screw head on top of the abutment led to lower stress values than when the screw was located inside the abutment.
4. A crown margin located incisal to the screw head resulted in increased stress at the cervical area of the abutment.

### References

1. Albrektsson T. The response of bone to titanium implants. CRC Crit Rev Biocomp 1984;1:53–84.
2. Albrektsson T, Zarb G, Worthington P, Eriksson AR. The long-term efficacy of currently used dental implants: A review and proposed criteria of success. Int J Oral Maxillofac Surg 1986;1:11–25.
3. Davis DM. The role of implants in the treatment of edentulous patients. Int J Prosthodont 1990;3:42–50.
4. Papavasiliou G. Finite Element Analysis of Stress-Induced Fractures in Bone Around Dental Implants [Master's thesis]. Chapel Hill, NC: University of North Carolina, 1992:87–89.
5. Newman MG, Flemming TF. Periodontal considerations of implants and implant-associated microbiota. J Dent Educ 1988;52:737–744.
6. Tripodakis APD, Strub JR, Kappert HF, Witkowski IS. Strength and mode of failure of single implant all-ceramic abutment restorations under static loads. Int J Prosthdont 1995;8:265–272.
7. McLean JW. The Science and Art of Dental Ceramics, vol I. The Nature of Dental Ceramics and Their Clinical Use. Chicago: Quintessence, 1979:133–140.
8. Pröbster L. Survival rate of In-Ceram restorations. Int J Prosthodont 1993;6:259–263.
9. Jemt T, Carlsson L, Boss A, Jörnéus L. In vivo load measurements of osseointegrated implants supporting fixed or removable prostheses: A comparative pilot study. Int J Oral Maxillofac Implants 1991;6:413–417.
10. Schmitt SM, Chance DA. Fabrication of titanium implant-retained restorations with non-traditional machining techniques. Int J Prosthodont 1995;8:332–336.
11. Olarn RC, Lacefield WR. The passive fitting implant restoration. Implant Soc 1993;4:8.
12. Eidenbenz S, Lehner CR, Scharer P. Copy milling ceramic inlays from resin analogs: A practicable approach with the CELAY system. Int J Prosthodont 1994;7:134–142.
13. Rieger MR, Mayberry M, Brose MO. Finite element analysis of six endosseous implants. J Prosthet Dent 1990;63:671–676.

14. Williams KR, Watson CJ, Murphy WM, Scott J, Gregory M, Sinobad D. Finite element analysis of fixed prostheses attached to osseointegrated implants. Quintessence Int 1990;21:563–570.
15. Kamposiora P, Papavasiliou G, Bayne SC, Felton DA. Finite element analysis estimates of cement microfracture under complete veneer crowns. J Prosthet Dent 1994;71:435–441.
16. Timoshenko S, Young DH. Elements of Strength of Materials, ed 5. New York: Van Nostrand–Reinhold, 1968:377.
17. Peters MCRB, Poort HW. Biomechanical stress analysis of the amalgam–tooth interface. J Dent Res 1983;62:358–362.
18. Carter DR, Spengler DM. Mechanical properties of cortical bone. Clin Orthop Rel Res 1978;135:192–217.
19. Knoell AC. A mathematical model of an in vivo human mandible. J Biomech 1977;10:59–66.
20. Huysmans MCDNJM, Van der Varst PGT. Finite element analysis of quasistatic and fatigue failure of post and cores. J Dent 1993;21:57–64.
21. Farah JW, Craig RG. Finite element stress analysis of a restored axisymmetric first molar. J Dent Res 1974;53:859–866.
22. McLean JW, Hughes TH. The reinforcement of dental porcelain with the ceramic oxides. Br Dent J 1965;119:251–267.
23. McComb D, Sirisko R, Brown J. Comparison of physical properties of commercial glass-ionomer luting cements. J Can Dent Assoc 1984;9:699–701.
24. Manufacturer's Information. Bad-Säckingen, Germany: Vita Zahnfabrik, 1994.
25. Craig RG. Restorative Dental Materials, ed 6. St Louis: Mosby, 1980;79:331.

*Literature Abstract*

## Microscopic evaluation of bone-implant contact between hydroxyapatite, bioactive glass, and tricalcium phosphate implanted in sheep diaphyseal defects

A principal concern of investigators studying material implantation is whether direct contact of the implant with living bone is achieved. This study compared the histomorphology of the bone-implant interfaces between host bone and three implanted ceramic materials, hydroxyapatite (HA), bioactive glass (BG), and tricalcium phosphate (TCP). To compare the interfaces between ceramic implants and host bone in vertebrates, 20 × 20 mm cylinders of HA (Cremascoli, Milan, Italy), BG (prepared according to the Hench procedure as modified by Pazzaglia et al) and TCP (B247, DePuy, Warsay, IL, USA) were implanted in segmental defects of the tibia of 18 adult sheep. The sheep were killed 16 weeks after implantation. Three types of visible bone-implant contacts were identified microscopically. The trabecular weblike bone–implant contact noted with tricalcium phosphate seemed superior to the disseminated patchy bone-implant contact with bioactive glass and the buttressed bone-implant contact with hydroxyapatite in regard to both bone ingrowth and bioresorption of the implant material. A larger amount of remodeled bone was observed around TCP implants than around HA or BG implants. No inflammatory reactive cells were observed on the interface between any of three ceramic implants and bone. The authors concluded that the microscopic differences in the bone-implant interfaces between HA, BG, and TCP were chiefly determined by they physicochemical properties on the surface of the materials themselves. Furthermore, the mechanical strength, geometry, and porosity of implantable ceramic materials should also be considered before the materials are introduced for clinical application.

**Gao TJ, Lindholm TS, Kommonen B, Ragni P, Paronzini A, Lindholm TC.** *Biomaterials* 1995;16(15):1175–1179. **References:** 26. **Reprints:** T.J. Gao, Bone Transplantation Research Group, Department of Clinical Medicine, University of Tampere, P.O. Box 607, FIN-33101, Tampere, Finland.—*Richard R. Seals, Jr, DDS, MEd, MS, Department of Prosthodontics, The University of Texas Health Science Center at San Antonio, San Antonio, Texas*